Acta Scientific Pharmaceutical Sciences (ISSN: 2581-5423)

Volume 7 Issue 9 September 2023

Review Article

Investigation of the $CaCO_3$ Impact on Both the Annealing Temperature and Mechanical Properties of Microporous Films that Were Obtained Through a Single Extrusion Process

Kian Habibi[1-3]*, Soleiman Mosleh[3], Antonio B Martínez[1], Kiavash Habibi[2] and David Arencón[1]

[1]Centre Català del Plàstic, Universitat Politècnica de Catalunya, Barcelona, Spain

[2]Kian Paniz Industry, Scientific and Technology Park, Gachsaran, Iran

[3]Polymer Engineering Department, Gachsaran Faculty of Petroleum and Gas, Yasouj University, Gachsaran, Iran

***Corresponding Author:** Kian Habibi, Professor, Centre Català del Plàstic, Universitat Politècnica de Catalunya, Barcelona, Spain.

Received: August 03, 2023

Published: August 18, 2023

Abstract

Calcium carbonate in micron size was opted for the fabrication of microporous membranes based on polypropylene through the MEAUS approach (melt extrusion-annealing-uniaxial stretching) and a twin-screw extruder. Polypropylene was blended with different amounts of fillers (1, 5, 10% by weight calcium carbonate). Various techniques were employed to examine the effects of the fillers. The crystal orientation was analyzed using polarized infrared spectroscopy (FTIR), while differential scanning calorimetry (DSC) was used to investigate crystal properties. The thermal stability of the membrane was evaluated using thermogravimetric analysis (TGA). Tensile testing was done to determine the rigidity and ductility of the produced types. The use of mineral fillers resulted in an enhanced pore distribution across the surface of the membrane. The mechanical results suggested that the formation of micropores is likely to occur more easily in the amorphous phase, as annealing leads to the perfection of lamellae and the reduction of molecular chain entanglements in the amorphous phase.

Keywords: Microporous Membranes; Annealing Temperature; Amorphous Tie Chains; Tensile Test

Introduction

The use of membranes has become increasingly common in a wide range of applications and serves various purposes across multiple industries. These applications include separation processes and chemical technology, among others, and come in a variety of shapes and forms. One particularly important characteristic of membranes is their capacity to regulate the rate of permeation of different species. Oftentimes, this property is harnessed to achieve effective separation of chemical substances through the membrane [1]. Additionally, membranes are also employed in critical first-stage operations, such as separating well-stream gas from free liquids. For this specific application, the desired type and size of the separator are determined by the composition of the fluid mixture and pressure [1,2].

Polymeric membranes can be fabricated utilizing a range of techniques, including phase separation, track etching, leaching, thermal precipitation, and stretching. The process of phase inversion involves mixing the polymeric raw material with a solvent and non-solvent, where phase separation leads to the formation of a matrix in the first phase rich in polymer and the creation of pores in the second phase of the polymer. Track etching employs

irradiation of the polymeric film that is subsequently acid-etched to create tracks. Leaching involves extruding a solid particle-filled polymeric raw material, followed by the extrusion of the solid, leading to porosity formation [1-3]. Thermal precipitation involves the cooling of a mixture comprising a polymer and solvent, resulting in phase separation, which subsequently leads to solvent extrusion. The stretching method utilized in this process is centered on the extension of a polymer film that contains a dispersed phase. This stretching causes the creation of stretching pores due to stress concentrations at the interface of these sites or the stretching of specific crystalline morphology [1-5]. Phase separation is the most commonly used technology for manufacturing polymeric membranes. Nonetheless, two environmental challenges associated with solution casting, namely solvent contamination and the expensive cost of solvent recovery, must be taken into consideration. Despite these concerns, substantial progress has been made in the past decade to improve the situation.

In the course of this study, the technique of MEAUS (melt extrusion–annealing– uniaxial strain) was implemented as a means of polymer stretching. This method applies to semi-crystalline polymers and involves the following series of steps: (1) the stretching of a thin film with a row nucleated lamellar structure, (2) annealing of the film to thicken the lamellae, and (3) the stretching of the film at a low temperature to create voids, followed by stretching at high temperature to enlarge the pores. Given the delicate nature of the extrusion and production process required for the precursor films, it is imperative that samples should be produced under a high draw ratio and cooling rates to achieve a uniformly thick film, as any non-uniformity or thickness variation could lead to stress distribution irregularities. From a financial standpoint and an environmental one, the MEAUS method proves relatively cost-effective and does not pose the risk of solvent contamination. One issue that arises in the technology and industrial market of these products is the challenge of achieving a homogenous distribution of pore morphology during fabrication. Additionally, another limitation is the narrow range of polymers that can generate the initial row-lamellar structure. Among these polymers, polypropylene is the most commonly used option for producing microporous membranes via the MEAUS method. The stretching process involved in this method is also helpful for incorporating mineral fillers that aid in enhancing membrane performance [6,7]. Because of their exceptional chemical and mechanical resistance properties, polyolefins such as polypropylene find application in various separation processes, including gas/water filtration and lithium batteries [7,8].

Multiple studies have reported on the impact of polymer architecture on the creation of the row-nucleated structure required for the MEAUS method [2,9-11]. Among the works conducted in this area, the research groups of Ajji [5] and Caihong [11] stand out for their focus on the use of neat polyolefins. However, only a few studies have explored the use of filled polyolefins. For instance, Nakamura and Nago [9] introduced pores into the polymeric matrix by debonding the calcium carbonate and assessed the correlation between the stretching degree and properties of microporous polypropylene sheets. Similarly, Saffar., *et al*. [5,7] developed hydrophilic membranes made of polypropylene micropores and investigated changes in the crystalline structure and membrane performance to optimize annealing and stretching processes. Mineral fillers have been observed to confer increased rigidity and a more hydrophilic surface characteristic of membranes. Additionally, their presence can affect the final porous morphology, as many fillers exhibit nucleate ability in the crystallization process of polyolefins [7,9-13]. Notably, the largest current application of mineral fillers is in the production of CO_2 from flue gases emanating from gas-fired cogeneration plants, with the resulting CO_2 being re-used in greenhouses or as Enhanced Oil Recovery (EOR) at mature oil fields in the Gulf Coast region. The CO_2 capture plant itself is composed of pre-treatment, CO_2 absorption, regeneration, CO2 compression with dehydration, and a self-sufficient utility system [14].

The utilization of innovative absorption liquids and porous polyolefin membranes in membrane gas absorption presents an effective solution for eliminating sulfur dioxide emitted from a variety of burning flare gases. An assessment of its practicability indicates that the extraction of sulfur dioxide from flue gas can be achieved in a cost-efficient manner on a significant scale [15].

Within this study, a twin-screw extruder was used, with particular emphasis placed upon a novel modification of the extrusion process - namely, rapid air cooling, with introducing of calcium carbonate

as a mineral filler. A polypropylene material previously validated in works [6,7] - with various percentages of micro-sized calcium carbonate incorporated - was employed. Our investigation focused on the interplay between polymeric composition and membranes produced via the MEAUS technique, to assess the impact of calcium carbonate content on final membrane properties. Specific blends of varying calcium carbonate content yielded more uniform and larger pores in the membranes. Finally, extrusion temperatures were varied while maintaining a constant draw ratio to produce species composed of both neat polypropylene and its various blends. Moreover, different temperature values were employed during the annealing and stretching phases to investigate the impact of this variable on the development of porous morphology. Notably, extreme temperature values, close to the melting point, were utilized in some instances. The modifications occurring in the structure of the membrane were analyzed using various characterization techniques. A comprehensive assessment of the correlation between crystalline properties, porous morphology, permeability, and thermal and mechanical stability was conducted. This study endeavors to scrutinize the crystalline orientation, membrane morphology, thermal behavior, membrane permeability, and mechanical traits of the membranes, while examining the influence of the cold and hot strain phases of the MEAUS process on the mechanical properties of the membranes.

Experimental procedure

Materials

To conduct the study, a commercial extrusion grade named PP020 was procured from Repsol S.A located in Madrid, Spain. The melt flow rate of this material was measured to be 1.0 dg·min-1 at 230 °C and 2.16 kg. The analysis of the molecular characteristics revealed that the average number and mass molecular weights were Mn =119 kg·mol-1 and MW=659 kg·mol-1, respectively. The monomodal mass molecular weight distribution was observed in this grade. To get the desired properties, micro-sized ultrafine surface-treated precipitated calcium carbonate was incorporated as filler, with an average size of 4 μm. The sample was kindly supplied by Reverté Calcium Carbonates, a leading supplier of such minerals in Spain. Table 1 illustrates the relevant attributes of this selected mineral filler and the average size used in the investigation.

Tradename	Average size	Surface treatment
M95T	98.5%, 4 mm value 94.0 ± 2.0%	$MgCo_3$, Fe_2O_3, amino group, dispersible

Table 1: Calcium Carbonate Properties.

The production of film and preparation of its precursor materials

The films that precede the production of porous membranes are mono-oriented and have a row-lamellar structure. These precursor films are created during the melt-extrusion process, which is the first step of the MEAUS technique. Polypropylene/calcium carbonate pellets, comprising 1, 5, and 10 wt.% of calcium carbonate are denoted as C1 (99-1 wt.%), C5 (95-5 wt.%), and C10 (90-10 wt.%) in this study. They were produced through melt mixing using a co-rotating twin-screw extruder (Collin ZK-35, L/D = 36, Dr. Collin GmbH, Ebersberg, Germany) equipped with a 1.9 mm thickness and 25 mmwidth slit die (Figure 1). Additionally, precursor films (1, 5, and 10 wt.% calcium carbonate) made of polypropylene-calcium carbonate, referred to as C1 (99-1 wt.%), C5 (95-5 wt.%), and C10 (90-10 wt.%) in this study, were also produced using these pellets, with a constant rotating speed of 40 rpm. The effects of temperature on material properties during this stage were studied by producing samples at temperature profiles ranging from 180 to 240 ºC. Upon exiting the extruder, a die with a rectangular cross-section and nominal dimensions of 122 mm x 1.9 mm was fixed. The die was accompanied by a duo of air knives situated in close proximity to the die to swiftly cool the film surface at the point of exit. The film was then moved through a three-calander system that produced a nominal draw ratio of 70 for all samples, as depicted in Figure 2. The precursor films had a nominal thickness ranging between 25-35 mm.

Annealing and uniaxial stretching

Samples of rectangular shape were obtained from a preliminary film measuring 25 mm in thickness. The samples were cut to width and length of 60 and 100 mm, respectively. These samples were subjected to annealing without extension at three distinct temperatures (90, 115, and 140 ºC), using an air-circulating oven for 15 minutes.

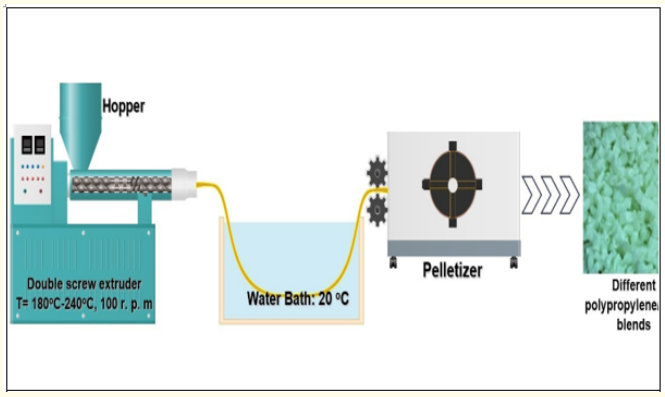

Figure 1: Process outlines for the compounding of polypropylene/$CaCO_3$ blends.

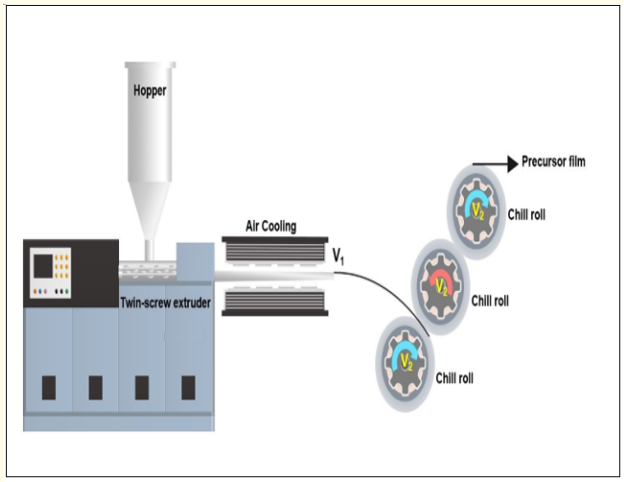

Figure 2: Process of the precursor film production and adjustment of air knives.

Consequently, the annealed precursor rectangular film samples underwent uniaxial strain testing on a Galdabini Sun 2500 universal testing machine, which was equipped with a 1 kN load cell and a climatic chamber. This process was carried out in two distinct stages. First, at room temperature, the samples were tested at a drawing speed of 50 mm/min until reaching 35% elongation at a cold stage. Second, in a hot stage, the samples were stretched at three varying temperatures (90, 115, 140 ºC) and a strain rate of 10 mm/min until they reached 230% of their initial length. The uniaxial strain was parallel to the precursor film's drawing direction during extrusion (MDO — machine direction orientation). Once the test was completed, and prior to the release of the films from the tensile grips, the membranes were held for 90 seconds at the same hot temperature to stabilize their porous morphology.

Membranes characterization

The Fourier-Transmission Infrared spectra were employed to evaluate the crystalline characteristics of the samples. The Perkin Elmer 1000 FTIR (Perkin Elmer, Waltham, MA, USA) infrared spectrometer, with a spectral resolution of 1 cm^{-1} and polarized beam, was utilized for this purpose. The crystalline orientation was assessed for both nonannealed and annealed samples, which were subjected to different temperatures. The difference in absorption in two orthogonal directions, parallel (A_0) and perpendicular (A_{90}) to the reference axis MD (extrusion machine direction), was used to determine the orientation. To determine the orientation of the crystalline phase (F_c), data were acquired from the range of 4000 to 600 cm^{-1} at the wavelength of 998 cm^{-1}. The Herman orientation function was calculated as per Equation (1):

$$Fc = (D - 1) / (D + 2) \text{ ---------(1)}$$

Where dichroic ratio (D) is the ratio of both absorbencies, parallel and perpendicular (A_0/A_{90}).

The membrane pore structure was analyzed through the use of Scanning Electron Microscopy with the JEOL JSM-7001F microscope, which operated at a voltage of 2 kV from JEOL in Akishima, Japan. Prior to analysis, the samples were coated with a thin layer of gold in an argon atmosphere using the BAL-TEC SCD005 Sputter Coater from BAL-TEC in Balzers, Liechtenstein. From multiple SEM micrographs taken for each sample, the surface morphology of the membranes was characterized, and the number of pores, pore area, and average pore size was measured in an image analysis program (Buehler Omnimet, version Omnimet Advanced, Buehler, Lake Bluff, IL, USA, 2015). It was assumed that a circular-diameter porous geometry was present for calculation purposes. The average pore density of the precursor films was then determined by dividing the number of pores by the membrane's surface area.

The examination of thermal characteristics and phase alterations from amorphous to crystalline states was conducted

using the differential scanning calorimetry (DSC Q1000, TA instruments, New Castle, DE, USA) method. Calibration of the equipment was accomplished by implementing standard samples containing indium and lead. For the examination, samples with an approximate mass of 5-7 mg were heated from 30 to 200 °C, at a rate of 10 °C/min. The crystallinity percentage of the samples was determined using Equation (2):

$X_m = (^{\Delta Hm}/\Delta H_m 0) \times 100$ -------- (2)

Where ΔH_m is the melting enthalpy measured in the resulting thermograms by integrating the area under the peaks (J/g) and $\Delta H_m^{\ 0}$ is the theoretical enthalpy of PP 100% crystalline (207.1 J/g).

The thermal stability of the membranes was assessed by conducting thermogravimetric analyses using a TGA/DSC 1 Mettler Toledo Star System from Mettler Toledo, Columbus, OH, USA. The samples, weighing approximately 8.0 mg, were subjected to a heating rate of 10 °C/min and heated from 40 to 1000 °C. Three separate analyses were conducted for each membrane using a constant air flow of 60 mL/min.

The air permeability of the porous membranes was quantified using the internationally recognized ISO 5636-5 standard and measured with a Gurley densimeter from Lorentzen & Wettre, ABB, Zurich, Switzerland. The Gurley value was calculated by determining the time (t) it took for a settled volume (100 mL) of air to pass through the sample with a fixed area (0.79 cm^2) under a pressure of 0.02 MPa. A longer Gurley value indicates lower air permeability and signifies a more convoluted path for air transportation through the pores. The Gurley permeability value was determined using the following equation:

Gurley permeability = 135.5 / t -----(3)

Porosity estimation of all the membranes was predicted by imbibition of the membranes into the water for 24 h using the grain volume method. Firstly, the dry weight of the samples (W_{dry}) and the saturated weight (W_{sat}) after imbibition were determined. The difference in weight is divided by the density of water (r_{water}) to find the pore volume (V_p) of samples as follows:

$V_p = (W_{sat} - W_{dry}) / \rho water$ --------(4)

Hence, using the density of the samples ($r_{objective}$) and applying Equation (5), it is possible to find the V_g value:

$Vg = W_{dry} / \rho objective$ ---------(5)

The percentage of porosity (F) was obtained by dividing the V_p by V_b as given in Equation (6):

$F = (V_p/V_b) \times 100$ (6) where V_b is the sum of V_p and V_g.

Mechanical characterization

For the assessment of mechanical properties along the machine direction (MD) of annealed precursor films, a universal tensile machine SUN2500 from Galdabini, Cardano al Campo (VA), Italy was utilized. The machine was equipped with a 1 kN load-cell and a video extensometer (MINSTRON OS-65D Minstron, Taipei, Taiwan). The mechanical tests were conducted at a strain rate applied during the first uniaxial stretching step, with tensile specimens stretched at room temperature and a constant speed of 50 mm/min. The obtained engineering stress-strain curves provided valuable information on the influence of polymer composition and annealing temperature on membrane performance.

Results and Discussion

The forthcoming section will cover four key topics, beginning with an exploration of the impact of extrusion and annealing temperature on neat polypropylene in Section 3.1. Subsequently, Section 3.2 will delve into the influence of annealing temperature on polymer blends. The effect of hot temperature in the uniaxial stretching step will be examined in Section 3.3, followed by an analysis of the influence of polymer composition and annealing temperature on the mechanical and thermal stability of membranes in Section 3.4.

The impact of the extrusion and annealing temperature on the properties of pure polypropylene

During the initial step of the MEAUS technique, it is feasible to regulate certain properties of precursor films that later transform into membranes in subsequent stages. Several variables associated with the melt extrusion process, such as draw ratio and air-cooling, have been previously studied to fix the crystalline structure. As part of the present investigation, a homopolymer resin of polypropylene and micro-sized ultrafine surfacetreated

precipitated calcium carbonate as a filler were chosen to explore the influence of processing temperature on these materials. The temperature profile from the hopper to die was maintained within a range of 180 to 240 °C for all the resins. The produced membranes with the homopolymer were annealed at 140 °C and the precursor films were subjected to DSC thermograms before and after the annealing process, along with the uniaxial stretching process. SEM micrographs of the membrane are illustrated in Figure 3.

Thermal analyses were employed to assess any potential microstructural modifications that may occur during the annealing and uniaxial stretching stages. Based on the DSC thermograms illustrated in Figure 3a-b, it can be observed that the presence of a lower-temperature shoulder from the primary melting peak is linked to the annealing of the precursor films. During this phase, a secondary crystalline structure formed between the amorphous and the main crystal lamellae. Higher annealing temperatures facilitate an increase in molecular mobility and a reorganization of the structure, resulting in the thickening of the lamellar structure and the reduction of irregularities. These details can be found in references [14-19]. The DSC curves presented in Figure 3c demonstrate that annealed membranes displayed a disappearance of the left shoulder, accompanied by a wider total area. This is attributed to the presence of a range of crystalline structures with varied lamellar thicknesses. Moreover, the melting temperature was observed to increase while a more intense right peak was recorded, which can be attributed to the molecular orientation induced by stretching. Pores were formed through the uniaxial stretching process while a greater lamellae separation led to an increase in pore size. The stable crystalline form achieved during this step resulted in the appearance of the right peak, attributed to the stretching of certain tie chains that promote the crystallization of interconnected bridges, bridging the main crystal lamellae and dividing the pores [2,3,7,10].

Regarding the neat resin extruded at different temperatures, the endothermic curves demonstrated similar characteristics, as outlined in Table 2. The primary disparities may be observed in the SEM micrographs captured from the surface of the membranes, as well as in the data presented in Table 2 and Table 3. Across all species, elevating the annealing temperature of precursor films resulted in a corresponding increase in the orientation factor as determined by polarized infrared spectroscopy (FTIR). This trend is due to an acceleration of the molecular restructuring kinetics towards a more condensed and stable secondary form, as elucidated in previous studies [10,18]. While homopolymer species extruded at the same draw ratio, our research indicates that elevated temperatures above 250 °C encourage the development of a row-nucleated structure with a comparatively lower orientation factor, thereby decreasing the porosity and permeability of the membranes [6].

Sample	Extrusion (°C)	Annealing (°C)	Fc	Xm (%)	Pore Density (Pores/mm^2)	Pores Area (%)	Average Pore Size (mm)	Porosity (%)	Gurley Permeability (mm/(Pa.s))
PP020	240	90	0.60	50.2	9.1	5.0	0.061	0.42	0.103
		115	0.63	51	8.6	4.9	0.063	0.44	0.104
		140	0.69	52.4	9.8	6.1	0.065	0.46	0.104

Table 2: Characteristics of neat resin extruded and annealed at different temperatures in terms of the orientation of precursor films, membrane crystallinity, pore morphology, and air permeability.

F_c		Neat PP
Non-annealed precu	rsor	0.52
Annealed precursor	90 °C	0.60
	115 °C	0.63
	140 °C	0.69

Table 3: Orientation analysis was carried out through polarized FT-IR for PP, obtained by a twin-screw extruder.

Upon comparing the micrographs of different samples, it is evident that the pore density value experiences a significant change. It is also notable that higher annealing temperatures lead to the production of larger pore sizes. This effect can be attributed to the fact that the polypropylene matrix, during uniaxial stretching at high temperatures, surpasses its melting point, resulting in enhanced lamellae separation and an increase in both pore size

and air permeability values. However, there exists a downside to this process as it leads to the development of non-uniform areas in membranes prepared with neat polypropylene, as is evident from the SEM images. In this regard, the current study aims to overcome this limitation by adding varying percentages of calcium carbonate in the homopolymer resin, thereby achieving homogenous membranes with increased permeability by augmenting the pore size. Thus, for neat resins, the optimum annealing temperature appears to be around 160 °C. An increase in temperature close to the melting point of polypropylene results in increased air permeability due to the expansion of the density, area, and size of pores. This phenomenon occurs as a result of the softening of the crystalline region and an escalation in flexibility within the amorphous phase in hightemperature conditions.

Precursor films morphology

During the stretching phase, the chain portion is transformed into the initial connecting bridges. This phenomenon bears some similarity to the melting of crystalline lamellae under tensile stress, followed by the re-crystallization process, where an oriented fibrillar structure is obtained (as detailed in reference [19]). Nilsson., *et al*. (2012) proposed that the connecting bridge expansion process takes place during stretching and that the presence of tie chains resulting from chain entanglements was relatively limited. The vast majority of tie chains were found near the entanglement areas. During annealing, certain chains located in the vicinity of the initial lamellae are involved in the crystallization process. The image depicts a typical folded chain lamellar assembly, where the frozen entanglement points are confined within the interlamellar amorphous region.

According to research conducted by Caihong., *et al*. (2013) [20], increasing the annealing temperature results in the formation of uniform connecting bridges and pore structures in the stretched microporous membrane. Caihong Lei's findings [21] further support this assertion and demonstrate that annealing facilitates an improvement in the lamellar structure due to the occurrence of melting and recrystallization behavior. The disappearance of secondary crystals during cold and hot stretching enables their conversion into initial connecting bridges, while the enhanced lamellar structure offers support for the scaffold of the pore structure. Both cold and hot stretching methods yield the best connecting bridge arrangement for the microporous membrane after annealing, resulting in a distinguishable difference in the lamellar structure. Specifically, the stable initial lamellae are improved, and additional weak secondary crystals are induced.

In relation to the hot strain phase, a study conducted by Zuo., *et al*. (2007) [22] established that elevated temperatures can lead to increased chain mobility which weakens the amorphous entanglement network significantly. This weakening of the network causes chain disentanglement during tensile deformation, reducing the constraints for tie chains. The loosened tie chains act as bridges when stretched, forming connecting bridges that contribute to the formation and stabilization of the pore structure. Consequently, various calcium carbonate-based compounds undergo MEAUS phase resulting in a precursor with porous morphology. This final stage involves a uniaxial stretching procedure conducted at room temperature, with a 50 mm/min stretch rate and a 35% strain, as shown in Figure 3. During this particular phase, it is expected that the lamellae present in the row-lamellar structure will be compelled to undergo separation, resulting in a larger length of the interconnecting bridges amidst the lamellae.

Consequently, this will cause amplified pore size.

The impact of annealing temperature on the properties of polymer blends

The investigation into the influence of annealing temperature on calcium carbonate-based compounds produced through twin-screw extrusion (as illustrated in Figure 4) revealed that a higher annealing temperature resulted in the secondary annealing peak shifting to a greater temperature. This observation suggests that the new stable crystalline structure formed through annealing has a more substantial lamellar thickness when annealed at a temperature of 140 ºC.

The emergence of a secondary peak in filled compounds for neat polypropylene annealed precursor films can be attributed to shifts caused by annealing at higher temperatures. However, the calcium carbonate exhibited varying behavior, differing from the case of nucleation activity. While there were no noteworthy differences observed in the intensity and temperature shifting of this annealing peak related to the filler content.

Examining the morphological changes resulting from annealing suggests that two competing processes take place. Crystallites or fragments of them may undergo melting, giving rise to the development of new crystallites from the molten phase. At the same time, the thickening process is ongoing and involves segments of the original crystals, the predominance of which depends on molecular weight distribution, crystallization temperature, heating rate, and annealing temperature [20,23-25].

It can be concluded that the disparity between the endothermic curves regarding the crystallinity of non-annealed and annealed precursor films shows the gradual melting of less stable micro-crystallites, while simultaneously developing new crystallites that are thicker and/or more stable. As a result, the endothermic melting process is compensated by a re-ordering process. Notably, the annealed precursor films containing calcium carbonate exhibit greater levels of crystallinity compared to non/annealed precursor films. Furthermore, it is noteworthy that the addition of filler content did not significantly influence the crystallinity of annealed precursor films.

The impact of the elevated temperature used during the process of uniaxial stretching

An examination was conducted on the impact of hot stretching temperature on microporous membranes made from blends containing homopolymers and calcium carbonate. The study comprised utilizing three varying temperatures to enhance pore size and air permeability. All samples exhibited parallel behaviors, therefore, only findings relevant to the PP/C1 sample are displayed in Figure 4 and Table 4. These outcomes demonstrate that an increase in temperature higher than 140°C during the second uniaxial stretching phase results in larger pore size and longer recrystallized connecting bridges between lamellae. High temperatures allow for an increase in the flexibility of tie chains located in the amorphous phase, as well as the melting of ethylene content that exists in the PP matrix, thereby resulting in greater lamellar separation and the enhancement of pore size. An increase in pore size was observed in association with the collapse of neighboring pores when the interconnected bridges were ruptured because of high elongation values. This resulted in greater average pore size, but reduced pore density [14,21]. Nevertheless, it should be noted that excessive temperatures approaching the melting point of the material may induce local melting of the plastic, subsequently hindering membrane performance.

The impact of both polymer composition and annealing temperature on the mechanical and thermal durability of membranes

During the film stretching process in all samples, it was observed that a stress-withering phenomenon occurred [22]. However, no necking was observed, a behavior that is typically associated with a row-nucleated structure. Notably, two significant points were observed in the test results - the "first yield point" and the "second yield point," as depicted in Figure 5 [26]. The first yield point is characterized by the combination of fine chain slipping with a transformation that leads to a rearrangement within the lamellae, ultimately oriented in the stretching direction without breaking. On the other hand, the second yield point may be attributed to the deformation of the second crystalline lamellae. After the yield points, the tensile curves indicated a rise in nominal stress, signifying the beginning of the strain-hardening phenomenon.

The application of stress involved a preliminary arrangement of the amorphous tie chains prior to the unfolding of the crystal chain, which is commonly associated with the first yield point [27]. Conversely, the strain hardening of the second yield point has been linked to the deformation of the second crystalline lamellae formed during the annealing process. In terms of pore morphology, the initiation of micropore formation in the amorphous area corresponds to the first yield point, while the disruption of the lamellar structure corresponds to the second yield point. Notably, the lamellae are stretched apart along the tensile direction between these two yield points, as reported by Samuels (2013) [23]. Furthermore, the slope between the first and second yield points plays an important role in the stretching process. An increase in this slope has been associated with the separation of the lamellae rather than their interlamellar slippage during stretching [25].

Effect of annealing temperature

As previously mentioned, an investigation was carried out to evaluate the impact of annealing temperature on calcium carbonate/polypropylene blends (refer to Figure 6). The findings demonstrated that a rise in annealing temperature primarily resulted in a reduction of the initial yield point values (see Table 5). Notably, this pattern is in contrast to the observations made by Saffar (2014) for pure polypropylene [27], but is consistent with those reported by Caihong (2013) for neat polypropylene [21].

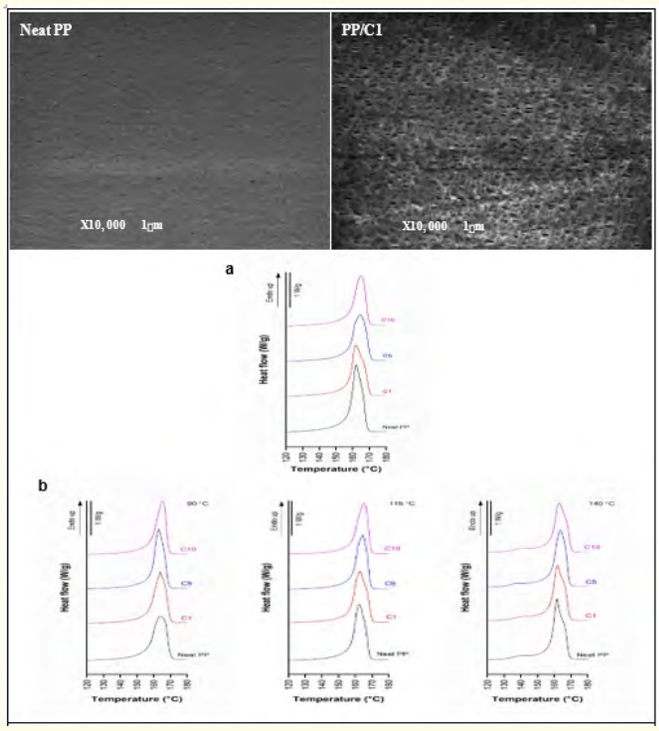

Figure 3: The present study features the application of scanning electron microscopy (SEM) to investigate different melting endotherms of PP/calcium carbonate compounds and neat PP. This was performed via a) the analysis of precursor films and b) annealed precursor films generated through a twin-screw extruder at varying temperatures of 90°C, 115°C, and 140°C.

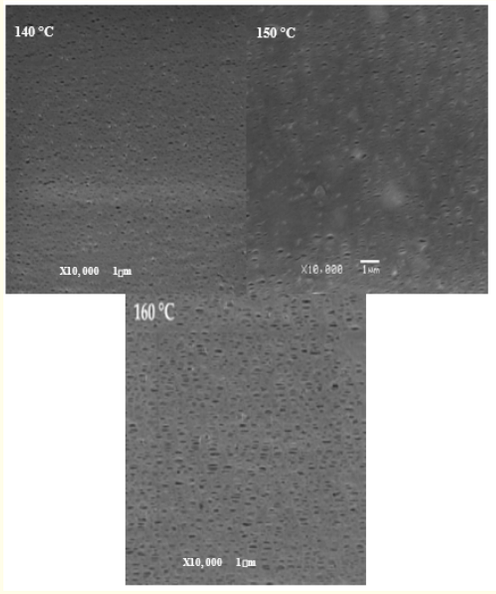

Figure 4: The current content showcases SEM micrographs of the PP/C1 sample, wherein the precursor films were subjected to annealing at 160°C and uniaxial stretching at three distinctive temperatures during the second stage.

Sample	Annealing (°C)	Hot Stretching (°C)	Xm (%)	Pore Density (Pores/mm²)	Pores Area (%)	Average Pore Size (mm)	Porosity (%)	Gurley Permeability (mm/(Pa.s))
PP/C1	160	140	54.1	28.7	12.6	0.089	1.96	0.189
		150	54.2	18.6	13.8	0.095	1.65	0.091
		160	55.0	13.5	11.1	0.099	1.21	0.089
PP/C1	160	140	54.1	28.7	12.6	0.089	1.96	0.189
		150	54.2	18.6	13.8	0.095	1.65	0.091

Table 4: The distinctions in membrane characteristics regarding crystallinity, pore morphology, and air permeability that arise from the manipulation of temperatures during the second stretching step are of interest.

The findings presented by Nitta and Takayanagi (2000) [28] demonstrate a clear correlation between mechanical properties and the fraction of tie chains in the amorphous region. Subsequent research has revealed that the decrease in yielding point after annealing can be attributed to the disappearance of certain tie chains which undergo crystallization [29]. This phenomenon suggests the occurrence of secondary crystallization during annealing, a conclusion that has been reached by other scholars as

well. Moreover, empirical data reveals that increasing the annealing temperature from 90 °C to 140 °C can result in a greater reduction in the yielding point, suggesting that secondary crystals continue to form.

The analysis of the C10 sample reveals that the slope between the first and second yield points at various annealing temperatures is higher than that of the precursor film. Moreover, the impact of annealing temperature on the stiffness of the films is significant, evident from the data in Table 5, which indicates a noticeable decrease across most cases as the temperature is increased. It is worth noting that annealing augments the size and quantity of lamellae, resulting in the precursor films presenting higher elongation at break compared to the annealed films.

Effect of filler addition

The investigation of annealed precursor films consisting of pure polypropylene versus calcium carbonate/polypropylene composites has been conducted and the findings have been presented in Figure 7 in the form of engineering stress-strain curves. The outcomes pertaining to the elastic modulus and first yield point have been compiled in Table 5, where it was observed that a convergence of two factors had an impact. While the first yield point of polypropylene was one of the lowest for all the materials examined, thus facilitating pore creation, the total elongation at break in the annealed precursor films of pure polypropylene was more restricted than in those of the filled variety. This indicates that the stage of stable pore growth was enhanced with the addition of filler to the polypropylene matrix, a conclusion that is further supported by the measured values of pore density and porous area in filled systems. Observations show that there are no noteworthy variations in the gradient regarding the initial and secondary stress points between polypropylene samples filled and unfilled. These findings provide evidence that a rational sequence of enhancement in the elastic modulus appears upon including calcium carbonate compounds as fillers.

In order to examine the impact of blending ratio and annealing temperature on the thermal stability of membranes, a thorough investigation was conducted via thermogravimetric analysis (TGA) and its derivative, DTG, for both neat polymers and their blends. Through the analysis of Figure 8 and subsequent collection of values

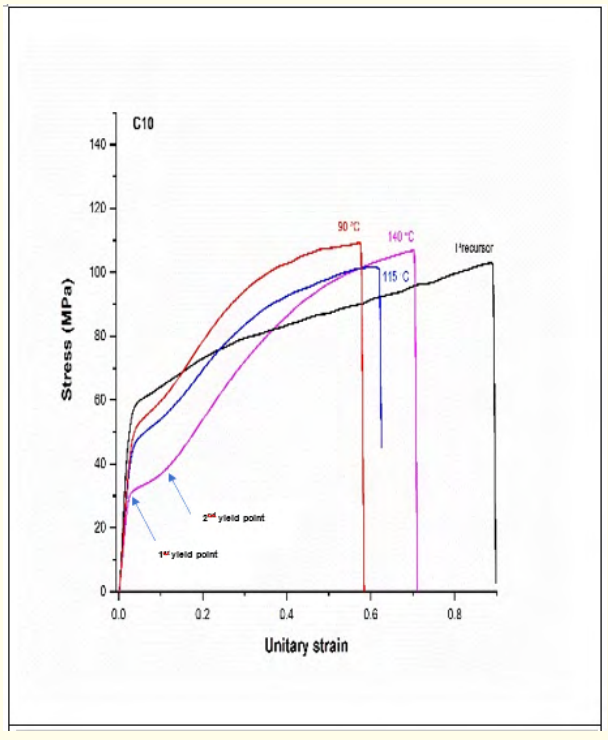

Figure 5: The stress-strain behavior of both unannealed precursor film and precursor films subjected to annealing at three distinct temperatures are displayed, highlighting the occurrence of the 1st and 2nd yield points.

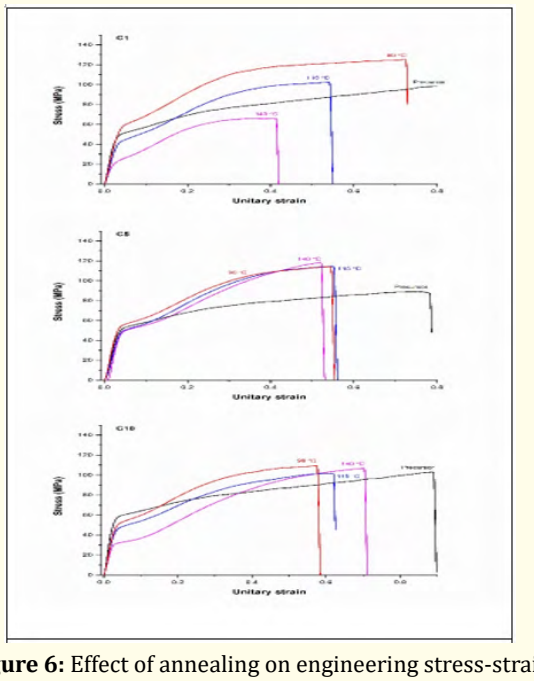

Figure 6: Effect of annealing on engineering stress-strain curves of PP/calcium carbonate precursor films.

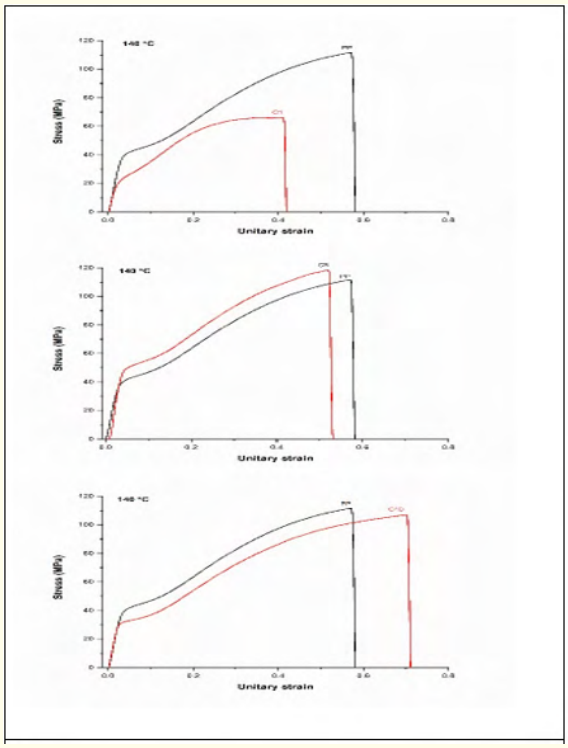

Figure 7: Effect of filler content on engineering stress-strain curves of PP/calcium carbonate annealed precursors.

outlined in Table 6, critical information was obtained, including the temperature required for a loss of mass of 10 wt % ($T_{0.1}$), 50 wt % ($T_{0.5}$), relative mass loss at 400 and 600°C, and the maximum decomposition rate temperature (T_{max}). For polypropylene, a range of reactions, including initiation, propagation, and termination, were identified as part of its thermal degradation mechanism. Ultimately, all TGA curves were characterized by a onesingle stage of decomposition, with the loss of mass being the only decomposition variable considered [6,8,22,23,25-27,30].

The experimental plots for filled membranes show a clear first-order mechanism that can be described by a one-single-step process, with the sole variable being the conversion of mass into volatiles [31-34]. This finding is supported by the detection of a single peak in DTG curves. The DSC results for calcium carbonate membranes suggest that a reduced amorphous phase is a contributing factor to heightened thermal stability in this type of membrane. These observations hold significant implications for optimizing the design and performance of such membranes.

	$CaCO_3$ wt. %	E (MPa)				1st Yield point (MPa)			
		Non-annealed.		Annealing temperature °C		Non-annealed. precursor film	Annealing temperature °C		
		Precursor film	90	115	140		90	115	140
Neat PP		1478	1235	1105	820	43	51	40	22
PP/$CaCO_3$	1	1802	1645	1413	859	57	53	41	22
	5	1701	1588	1498	1076	51	45	46	41
	10	1733	1717	1224	1146	47	44	50	42

Table 5: Elastic modulus and 1st yield point of the non-annealed and annealed precursor of PP/calcium carbonate.

Membrane	T0.1 (ºC)	T0.5 (ºC)	Lost mass 400ºC (%)	Lost mass 600ºC (%)	Tmax (ºC)
Neat PP	311.9	378.8	72.2	100.0	400.2
C1	304.8	365.4	83.8	99.4	394.9
C5	303.1	371.7	77.2	95.2	394.9
C10	302.9	388.0	62.5	91.3	405.0

Table 6: Thermal stability analysis of PP/calcium carbonate membranes.

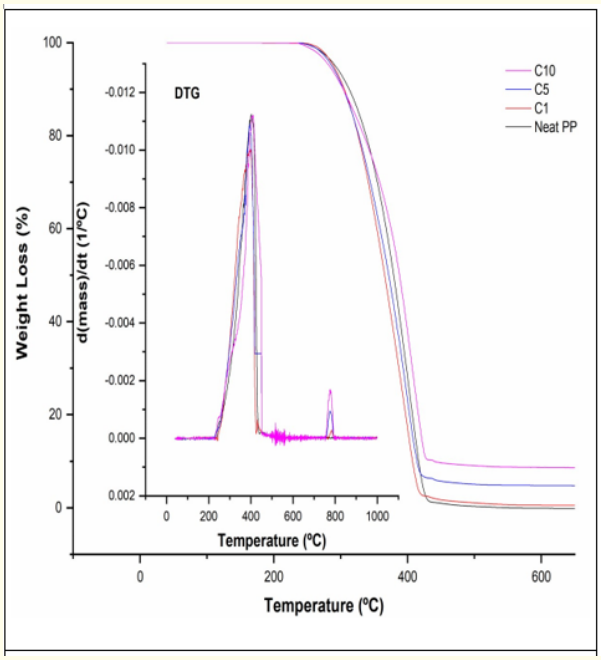

Figure 8: The thermogravimetric analysis (TGA) plots depicting the behavior of PP/calcium carbonate membranes were examined.

Conclusions

In this study, we conducted a comprehensive analysis of the polymer composition and temperature variation, including melt extrusion, annealing, and the second stage of uniaxial stretching, throughout the main phases of the MEAUS method. Our research focused on examining the mechanical properties of microporous films made from polypropylene filled with calcium carbonate. To enhance stiffness and mechanical properties, we used different weight percentages of calcium carbonate. Our findings, as demonstrated by results from tensile testing, table 5, and Figures 6-7, reveal the impact of varying calcium carbonate concentrations on performing the microporous films.

Various tests were conducted on PP/$CaCO_3$ samples containing different weight percentages at different temperatures. The values obtained for the 1st yield point and elastic modulus were calculated. Mechanical values of the filled annealed calcium carbonate films were presented in Table 5, including different contents of calcium carbonate with a strain rate of 50 mm/min. The results showed a considerable improvement in the mechanical values at 10 wt. % of calcium carbonate content compared to the neat PP film. Predictably, the increase in the modulus may be attributed to incorporating fillers in the polypropylene matrix, which exerted an impact on each particle by inducing stress concentration. As a result, if these areas merge and create a percolation network, the distance between particles would be minimized, thereby enhancing the modulus.

Furthermore, it should be noted that an increase in the total volume affected and a decrease in the inter-particle distance are observed when fine and well-dispersed particles are utilized at constant filler loadings. As a result of this phenomenon, the percolation network tends to develop more easily, thereby leading to an increase in the modulus. In light of this, Figure 5 presents the stress-strain curves of the PP/$CaCO_3$ precursor film that was extruded, as well as those annealed at temperatures of 90, 115, and 140 °C for 15 minutes. Notably, the annealed films exhibited a noteworthy difference in comparison to the as-extruded polypropylene precursor film, with two distinct yield points being evident in their stress-strain curves. Specifically, while the first yield stress and strain levels indicated a decline that could be attributed to the annealing temperature, the second yield stress and strain levels increased. Additionally, the curve slope between the two yield points demonstrated continuous amplification.

The initial and secondary yield points are indicative of micropore formation in the amorphous region and disruption of the lamellar structure, respectively, while the lamellae undergo stretching along the tensile direction. This phenomenon is supported by various references [25,35-39]. As such, the results indicate that the formation of micropores is more pronounced in the amorphous phase, while the ability of the lamellae to withstand damage strengthens as the films are subjected to higher annealing temperatures. This can be attributed to the improvement of lamellar perfection resulting from annealing, as well as a reduction in molecular chain entanglements in the amorphous phase. Furthermore, the increased slopes in the curves observed during annealing suggest greater lamellar separation, rather than interlamellar slippage, during the stretching process [6,8,16,17,25,29,34,35,40-43].

The experimental assessment encompassed the application of mechanical testing protocols on various annealed films composed of PP/$CaCO_3$ exhibiting discrete weight percentages of calcium carbonate (1, 5, 10 wt. %). Our findings demonstrate that the mechanical properties of PP/$CaCO_3$ films are enhanced with an elevation of calcium carbonate content up to 10 wt. %. Specifically, there was a noteworthy increase in modulus values, which may be attributed to the inclusion of fillers in the polypropylene matrix surrounding each particle, ensuring an impact on stress concentration.

The results of our study suggest that the formation of micropores tends to happen more easily in the amorphous phase since annealing enhances the perfection of the lamellae and reduces the molecular chain entanglements in the amorphous phase. Furthermore, the ability of the lamellae to resist damage strengthens the films annealed at higher temperatures, making it more impervious to damage. Furthermore, the heightened inclinations of the curves observed after annealing indicate that during the stretching operation, lamellar separation becomes more prevalent, rather than interlamellar slippage.

Acknowledgments

The authors would like to acknowledge Kian Paniz Industry for the financial support of project.

Bibliography

1. Baker RW. "Membrane Technology and Applications, Second Edition". Membrane Technology and Research, Inc. Menlo Park, California, US (2004).

2. Guiver M D and Lee YM. "Polymer rigidity improves microporous membranes". *Science* 339.6117 (2013): 284-285.

3. Sadeghi F., *et al*. "Analysis of microporous membranes obtained from polypropylene films by stretching". *Journal of Membrane Science* 292.1-2 (2007): 62-71.

4. SH Tabatabaei. "Development of microporous membranes from PP/HDPE films through cast extrusion and stretching". Ph.D. Dissertation, Université de Montréal, Montreal, Canada (2009).

5. Sadeghi F., *et al*. "Microporous membranes obtained from polypropylene blends with superior permeability properties". *Journal of Polymer Science Part B: Polymer Physics* 46.2 (2007): 148-157.

6. Castejón P., *et al*. "Polypropylene-Based Porous Membranes: Influence of Polymer Composition, Extrusion Draw Ratio and Uniaxial Strain". *Polymers* 10 (2017).

7. Habibi K., *et al*. "Effect of filler content, size, aspect ratio and morphology on thermal, morphological and permeability properties of porous talc filled-Polypropylene obtained through MEAUS process". *Advances in Polymer Technology* (2018).

8. Habibi K., *et al*. "The Comparison and Evaluation of Thermal Behavior, Pore Morphology, Permeability Properties, and Tensile Behavior Effects on Melt Stretching Calcium Carbonate/ Talc- Polypropylene-Based Microporous Membranes". *United Journal of Nanotechnology and Pharmaceutics* 1.1 (2021): 1-11.

9. S Nakamura., *et al*. "Microporous polypropylene sheets containing CaCO3 filler". *Journal of Applied Polymer Science* 49 (1993): 143150.

10. S Nagō., *et al*. "Microporous polypropylene sheets containing CaCO3 filler: Effects of stretching ratio and removing CaCO3 filler". *Journal of Applied Polymer Science* 68 (1998): 1543-1553.

11. L Caihong., *et al*. "The correlation between the lower temperature melting plateau endotherm and the stretching-induced pore formation in annealed polypropylene films". *Journal of Plastic Film and Sheeting* 28 (2012): 151-164.

12. Saffar PJ., *et al*. "Development of polypropylene microporous hydrophilic membranes by blending with PP-g-MA and PP-g-AA". *Journal of Membrane Science* 462 (2014): 50-61.

13. Qaiss A., *et al*. "Porosity formation by biaxial stretching in polyolefin films filled with calcium carbonate particles". *Journal of Applied Polymer Science* 123.6 (2011): 3425-3436.

14. Zhang J., *et al*. "Study on the viscosity of polypropylene composites filled with different size and size distribution CaCO3". *Polymer Composites* 32.7 (2011): 1026-1033.

15. T Hirata., *et al*. "Current Status of MHI CO2 Capture Plant technology, 500 TPD CCS Demonstration of Test Results and Reliable Technologies Applied to Coal-Fired Flue Gas". ScienceDirect, Energy Procedia 63 (2014): 6120-6128.

16. Xanthos M., *et al*. "Melt processed microporous films from compatibilized immiscible blends with potential as membranes". *Polymer Engineering and Science* 42.4 (2002): 810-825.

17. Xanthos M., *et al*. "Melt processed microporous films from compatibilized immiscible blends with potential as membranes". *Polymer Engineering and Science* 42.4 (2002): 810-825.

18. Nilsson F., *et al*. "Modelling tie chains and trapped entanglements in polyethylene". *Polymer* 53.16 (2012): 3594-3601.

19. Li Shiguang., *et al*. "Hybrid Membrane/Absorption Process for Post-combustion CO2 Capture". Gas Technology Institute, Des Plaines, IL, United States (2013): 12-31.

20. Caihong L., *et al*. "Influence of heat-setting temperature on the properties of a stretched polypropylene microporous membrane". *Polymer International* 63.3 (2013): 584-588.

21. Caihong L., *et al*. "Formation of stable crystalline connecting bridges during the fabrication of polypropylene microporous membrane". *Polymer Bulletin* 70.4 (2013): 1353-1366.

22. Zuo F., *et al*. "The role of interlamellar chain entanglement in deformation induced structure changes during uniaxial stretching of isotactic polypropylene". *Polymer* 48.23 (2007): 6867-6880.

23. Samuels RJ. "High strength elastic polypropylene". *Journal of Polymer Science Part B* 17.4 (1979): 535-568.

24. Wang S., *et al*. "Fabrication of microporous membranes from melt extruded polypropylene precursor films via stretching: Effect of annealing". *Chinese Journal of Polymer Science* 33.7 (2015): 1028-1037.

25. Wang S., *et al*. "Fabrication of microporous membranes from melt extruded polypropylene precursor films via stretching: Effect of annealing". *Chinese Journal of Polymer Science* 33.7 (2015): 1028-1037.

26. Pae KD., *et al*. "Healing of stress-whitening in polyethylene and polypropylene at or below room temperature". *Polymer Engineering and Science* 40.8 (2000): 1783-1795.

27. Saffar A., *et al*. "The impact of new crystalline lamellae formation during annealing on the properties of polypropylene-based films and membranes". *Polymer* 55.14 (2014): 3156-3167.

28. Nitta KH and Takayanagi M. "Tensile yield of isotactic polypropylene in terms of a lamellar-cluster model". *Journal of Polymer Science Part B: Polymer Physics* 38.8 (2000): 1037-1044.

29. Liu D., *et al*. "Effect of annealing on phase structure and mechanical behaviors of polypropylene hard elastic films". *Journal of Polymer Research* 20.5 (2013): 1-7.

30. Franco-Urquiza EA., *et al*. "Effect of the strain rate and drawing temperature on the mechanical behavior of EVOH and EVOH composites". *Advances in Polymer Technology* 32.S1 (2013): 1-10.

31. Li Y., *et al*. "Polypropylene/calcium carbonate nanocomposites". *Polymer* 43.10 (2002): 2981-2992.

32. Diez F., *et al*. "Influence of the stretching in the crystallinity of biaxially oriented polypropylene (BOPP) films". *Journal of Thermal Analysis and Calorimetry* 81.1 (2005): 21-25.

33. Jiang G and Huang H. "Microstructure and Rheologic Development of Polypropylene/Nano-CaCO3 Composites along Twin-Screw Extruder". *Journal of Applied Polymer Science* 114.3 (2009): 1687-1693.

34. Ishikiriyama K and Wunderlich BK. "Crystallization and melting of poly (oxyethylene) analyzed by temperature-modulated calorimetry". *Journal of Polymer Science Part B* 35.12 (1997): 1877-1886.

35. Tabatabaei SH., *et al*. "Effect of processing on the crystalline orientation, morphology, and mechanical properties of polypropylene cast films and microporous membrane formation". *Polymer* 50.17 (2009): 4228-4240.

36. F Sadeghi., *et al*. "Analysis of row nucleated lamellar morphology of polypropylene obtained from the cast film process: effect of melt rheology and process conditions". *Polymer Engineering and Science* 47 (2007): 11701178.

37. Galeski A. "Strength and toughness of crystalline polymer systems". *Progress in Polymer Science* 28.12 (2007): 1643-1699.

38. Lei C., *et al*. "A study of plastic plateau disappearance in stress-strain curve of annealed polypropylene films during stretching". *Advances in Materials Research* 2 (2013): 111-118.

39. Tabatabaei SH., *et al*. "Microporous membranes obtained from polypropylene blend films by stretching". *Journal of Membrane Science* 325 (2008): 772-782.

40. Dong G and Lee Y M. "Microporous polymeric membranes inspired by adsorbent for gas separation". *Journal of Materials Chemistry A* 5.26 (2017): 13294-13319.

41. Wang Z., *et al*. "Microporous polymer adsorptive membranes with high processing capacity for molecular separation". *Nature Communication* 13 (2022): 4169.

42. Muldoon P F., *et al*. "Mixed Matrix Membranes from a Microporous Polymer Blend and Nano-sized Metal-Organic Frameworks with Exceptional CO2/N2 Separation Performance". *ACS Materials Letters* (2020).

43. Guo X., *et al*. "Mixed-Matrix Membranes for CO2 Separation: Role of the Third Component". *Journal of Materials Chemistry A* 7 (2019): 2473824759.